Additive-Free Synthesis of Poly(phenyleneoxide): Aerobic Oxidative Polymerization in a Base-condensed Dendrimer Capsule.

Kimihisa Yamamoto, Yuki Kawana, Masahiro Tsuji, Misa Hayashi, Takane Imaoka

Department of Chemistry, Faculty of Science and Technology, Keio University

E-mail: yamamoto@chem.keio.ac.jp

1. Preparation of Materials

Dendrimer ligands (**DPAG*n***: *n* = 1 ~ 4)[1] and the model compound[2] were synthesized as previously reported. Copper chloride anhydride (CuCl₂) and 2,6-difluorophenol were purchased from Aldrich as the reagent grade. All other chemicals and solvents were purchased from Kantoh Kagaku Co.

Chart S1. Chemical structures of the dendrimers and model compounds.

---
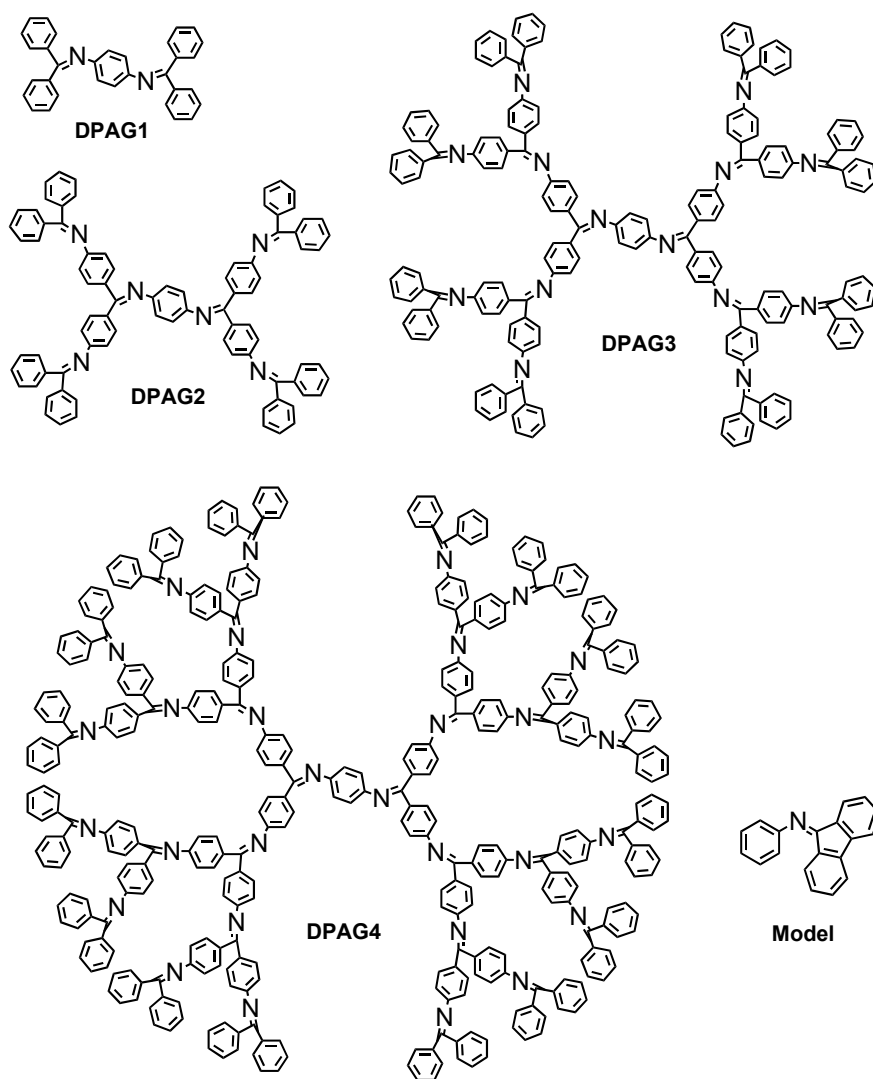
1 Takanashi, K.; Chiba, H.; Higuchi, M.; Yamamoto, K. *Org. Lett.* **2004**, *6*, 1709-1712.

2 Dai, W.; Srinivassan, R.; Katzenellenbogen, J. A. *J. Org. Chem.* **1989**, *54*, 2204-2208.

Supporting Information

2. Experimental Details of the Polymerization

Entry 1: DPAG4 (19.48 mg, 1/280 mmol) and $CuCl_2$ (0.96 mg, 1/140 mmol) were dissolved in a chloroform/acetonitrile (4 mL, v/v = 1/1) solution to form the complex (**2CuCl$_2$-DPAG4**). The solution was evaporated to dryness, and the solid was obtained. Polymerization of 2,6-difluorophenol (130 mg, 1 mmol) was carried out in chlorobenzene (2 mL) at 80 ˚C in the presence of the dendrimer complex under an O_2 atmosphere. After 72 h reaction, the mixture was cooled down and poured into methanol (400 mL) containing 5 % HCl. The precipitate was filtered and dried under vacuum at 60 ˚C. Finally, poly(2,6-difluoro-1,4-phenyleneoxide) (90.9 mg, 71 %) was yielded.
The normalized polymer yield (g_{PPO} mol_{Cu}^{-1} h^{-1}) was 177 g mol^{-1} h^{-1}. The number-averaged and weight-averaged molecular weight (Mw) was 5000 and 21300 respectively.

Entry 2: DPAG4 (9.74 mg, 1/560 mmol) and $CuCl_2$ (0.96 mg, 1/140 mmol) were dissolved in a chloroform/acetonitrile (2 mL, v/v = 1/1) solution to form the complex (**4CuCl$_2$-DPAG4**). The solution was evaporated to dryness, and the solid was obtained. Polymerization of 2,6-difluorophenol (130 mg, 1 mmol) was carried out in chlorobenzene (2 mL) at 80 ˚C in the presence of the dendrimer complex under an O_2 atmosphere. After 72 h reaction, the mixture was cooled down and poured into methanol (400 mL) containing 5 % HCl. The precipitate was filtered and dried under vacuum at 60 ˚C. Finally, poly(2,6-difluoro-1,4-phenyleneoxide) (104.9 mg, 82 %) was yielded.
The normalized polymer yield (g_{PPO} mol_{Cu}^{-1} h^{-1}) was 204 g mol^{-1} h^{-1}. The weight-averaged molecular weight (Mw) was 32,000.

Entry 3: PAMAM dendrimer G2 (5.81 mg, 1/560 mmol) and $CuCl_2$ (0.96 mg, 1/140 mmol) were dissolved in an acetonitrile (2 mL) solution to form the complex (**2CuCl$_2$-PAMAMG2**). The solution was evaporated to dryness, and the solid was obtained. Polymerization of 2,6-difluorophenol (130 mg, 1 mmol) was carried out in chlorobenzene (2 mL) at 80 ˚C in the presence of the dendrimer complex under an O_2 atmosphere. After 72 h reaction, the mixture was cooled down and poured into methanol (400 mL) containing 5 % HCl. However, no precipitate was obtained.

Entry 4: Pyridine (684 mg, 8.65 mmol) and CuCl (4.95 mg, 1/20 mmol) were dissolved in a chlorobenzene (2 mL). Polymerization of 2,6-difluorophenol (130 mg, 1 mmol) was carried out in the solution at 80 ˚C under an O_2 atmosphere. After 72 h reaction, the mixture was cooled down and poured into methanol (400 mL) containing 5 % HCl. The precipitate was filtered and dried under vacuum at 60 ˚C. Finally, poly(2,6-difluoro-1,4-phenyleneoxide) (59.7 mg, 46 %) was yielded.
The normalized polymer yield (g_{PPO} mol_{Cu}^{-1} h^{-1}) was 17 g mol^{-1} h^{-1}. The number-averaged and weight-averaged molecular weight (Mw) was 4380 and 9550, respectively.

Entry 5: Pyridine (684 mg, 8.65 mmol) and CuCl (0.71 mg, 1/140 mmol) were dissolved in a chlorobenzene (2 mL). Polymerization of 2,6-difluorophenol (130 mg, 1 mmol) was carried out in the

solution at 80 ˚C under an O_2 atmosphere. After 72 h reaction, the mixture was cooled down and poured into methanol (400 mL) containing 5 % HCl. However, no precipitate was obtained.

Entry 6: *N,N,N′,N′*-Tetramethylethylenediamine (5.81 mg, 1/20 mmol) and $CuCl_2$ (6.72 mg, 1/20 mmol) were dissolved in a chlorobenzene (2 mL). Polymerization of 2,6-difluorophenol (130 mg, 1 mmol) was carried out in the solution at 80 ˚C in the presence of excess 2,6-diphenylpyridine (115 mg, 1/2 mmol) under an O_2 atmosphere. After 72 h reaction, the mixture was cooled down and poured into methanol (400 mL) containing 5 % HCl. The precipitate was filtered and dried under vacuum at 60 ˚C. Finally, poly(2,6-difluoro-1,4-phenyleneoxide) (90.9 mg, 71 %) was yielded.

The normalized polymer yield (g_{PPO} mol_{Cu}^{-1} h^{-1}) was 25 g mol^{-1} h^{-1}. The number-averaged and weight-averaged molecular weight (Mw) was 2800 and 21300, respectively.

Entry 7: *N,N,N′,N′*-Tetramethylethylenediamine (0.83 mg, 1/140 mmol) and $CuCl_2$ (0.96 mg, 1/140 mmol) were dissolved in a chlorobenzene (2 mL). Polymerization of 2,6-difluorophenol (130 mg, 1 mmol) was carried out in the solution at 80 ˚C in the presence of excess 2,6-diphenylpyridine (115 mg, 1/2 mmol) under an O_2 atmosphere. After 72 h reaction, the mixture was cooled down and poured into methanol (400 mL) containing 5 % HCl. The precipitate was filtered and dried under vacuum at 60 ˚C. However, no precipitate was obtained.

Entry 8: *N,N,N′,N′*-Tetramethylethylenediamine (0.83 mg, 1/140 mmol) and $CuCl_2$ (0.96 mg, 1/140 mmol) were dissolved in a chlorobenzene (2 mL). Polymerization of 2,6-difluorophenol (130 mg, 1 mmol) was carried out in the solution at 80 ˚C under an O_2 atmosphere. After 72 h reaction, the mixture was cooled down and poured into methanol (400 mL) containing 5 % HCl. The precipitate was filtered and dried under vacuum at 60 ˚C. However, no precipitate was obtained.

Entry 9: Model (1.82 mg, 1/140 mmol) and $CuCl_2$ (0.96 mg, 1/140 mmol) were dissolved in a chlorobenzene (2 mL). Polymerization of 2,6-difluorophenol (130 mg, 1 mmol) was carried out in the solution at 80 ˚C under an O_2 atmosphere. After 72 h reaction, the mixture was cooled down and poured into methanol (400 mL) containing 5 % HCl. The precipitate was filtered and dried under vacuum at 60 ˚C. However, no precipitate was obtained.

3. Characterization of the Global Structure in a Dendrimer Complex

The metal binding process to **DPAG4** was examined as described below. First, 5 μmol l^{-1} solution of the **DPAG4** in a chloroform / acetonitrile (v/v = 1/1) mixed solvent (**Solution 1**) was prepared. The concentration of the **DPAG4** was optimized by the absorption intensity around 300 – 400 nm (absorption bands of the free dendrons). Dehydrated grade of the solvent was used as the solvent because an excess amount of water (H_2O) prevents stoichiometric complexation between $CuCl_2$ and the imine nitrogen. Second, the relatively concentrated solution (ca. 6 mmol l^{-1}) of $CuCl_2$ in acetonitrile (**Solution 2**) was prepared. The UV-vis absorption spectrum of **Solution 1** (3 ml) was

measured in a quartz cell (optical path length = 1 cm) sealed by a Teflon cap. The equimolar amount of $SnCl_2$ solution (**Solution 2**) was then added to **Solution 1**. This does not affect the total concentration of **DPAG4** and its complex in **Solution 1** because volume of the added **Solution 2** is much smaller than that of **Solution 1** (3 ml). Thus, the increase in the total solution volume in the UV cell could be negligible. The spectral changes after the addition of **Solution 2** to **Solution 1** converged within few minutes, and then the spectrum was recorded. The equimolar additions and the UV-vis spectra measurement processes were repeated until no spectral change was observed.
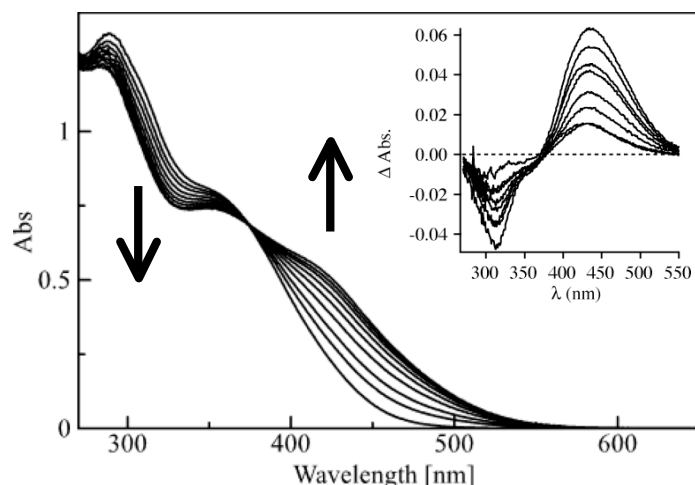

Figure S1. UV-vis spectral changes of **DPAG4** (5 µM) on the addition of $CuCl_2$ in $CHCl_3$ / CH_3CN. (Inset) Differential absorption spectra for each step of the titration.

During the titration, the wavelength of an observed isosbestic point appeared at ca. 370 nm gradually changed shorter. This observation was in good agreement with that reported previously using other metal chloride ($SnCl_2$, $FeCl_3$), suggesting stepwise complexation. The differential spectra (Figure S1. Inset) upon each drop were also gradually shifted to the shorter wavelength region. At first, the maximum absorption wavelength was observed at 438.5 nm, then shifted to 434.0 nm (8 eq.).

The copper species ($CuCl_2$) have lower affinity to the imines in DPAs. Thus, the complexation process cannot be directly determined by UV-titration method. In order to clarify the position of these metal complexes, we carried out ^{1}H NMR measurement. Upon the addition of paramagnetic metallic compounds, several proton signals near by the coordinating center drastically shifted due to the paramagnetic effect.[3,4] We actually found that the proton signals around 6.9-6.4 ppm, which is attributed as the inner phenyl protons of the dendron,[5] disappeared. In contrast, complexation with spin-less metal ($SnCl_2$) did not show such a disappearance although the signals became broader due to the metal exchange reaction within the timescale of NMR measurement. If the random complexation takes place, every proton should equally shift. These observations that specific signal decreasing strongly indicates selective binding to the layer nearest to the core. In our previous papers, the

3 Gorman, C. B.; Hager, M. W.; Parkhurst, B. L.; Smith, J. C. *Macromolecules* **1998**, *32*, 815-822.
4 Epperson, J. D.; Ming, L.-J.; Baker, G, R.; Newkome, G. R.; *J. Am. Chem. Soc.* **2001**, *123*, 8583-8592.
5 Higuchi, M.; Shiki, S.; Yamamoto, K. *Org. Lett*. **2000**, *2*, 3079-3082.

complexation of $FeCl_3$ is certificated in several analyses (UV-vis titration,[6] electrochemical measurement,[7] probing the core by redox potential and fluorescence[8]). The NMR analysis of $CuCl_2$ complexation supports similar manner of $FeCl_3$ complexation.
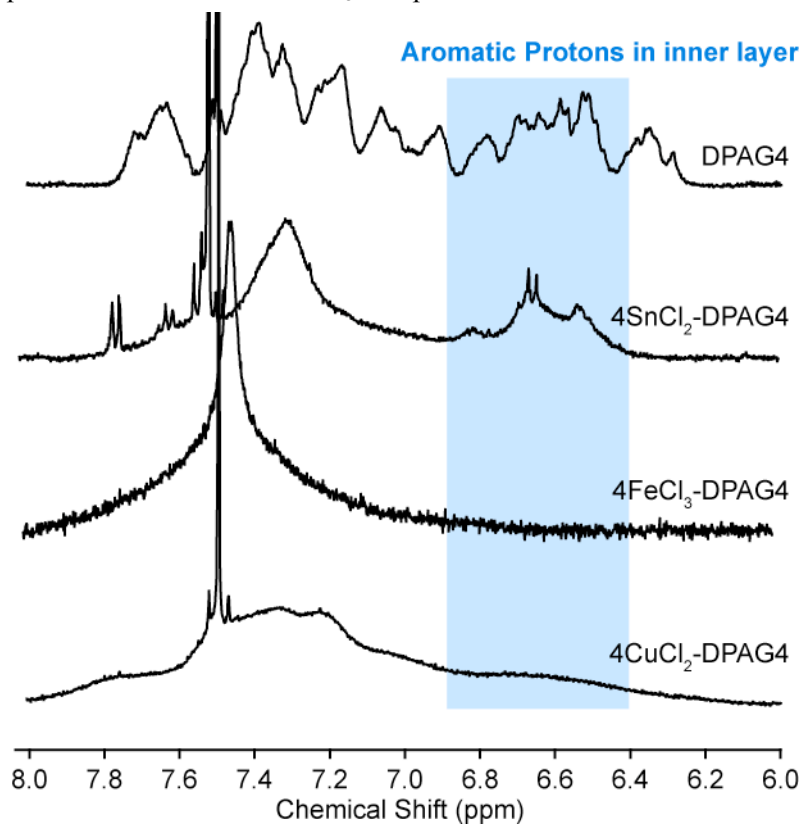

Figure S2. ^1H NMR spectra of free-DPAG4 and complexes.

4. Characterization of the Local Structure around a Copper Center

In order to elucidate the fine structure around the binding copper complexes, a crystal structure analysis was carried out. However, a single crystal of the **DPAG4** with copper complexes could not obtained due to its low crystallinity. Thus, we employed a model compound (Figure S3) of the DPA which has only one imine nitrogen. A single crystal of the complex (**CuCl₂-(Model)₂**) from the model compound and $CuCl_2$ was successfully obtained and the X-ray analysis was carried out.

Crystal data of the model complex (**1**), $C_{38}H_{30}Cl_4Cu_2N_2$, $M = 783.57$, triclinic, space group *P-1*, $a = 8.780(4)$ Å, $b = 9.284(6)$ Å, $c = 9.999(5)$ Å, $\alpha = 86.36(2)°$, $\beta = 73.37(2)°$, $\gamma = 86.97(2)°$, $U = 778.9(7)$ Å^3, $Z = 1$, $D_{calc} = 1.670$ g/cm^3, $\mu = 1.741$ mm^{-1}, crystal size 0.10 x 0.05 x 0.05 mm, 2758 reflections measured, $S = 3.172$, $R = 0.130$, and $R_w = 0.156$. Red prism crystals of **1** were obtained by the slow diffusion of hexane vapor into a chlorobenzene solution of **1**. A suitable crystal was mounted in a cryoloop. The intensity data were collected at 223.1 K on a Rigaku RAXIS-RAPID diffractometer with graphite monochromatized Mo Kα radiation ($\lambda = 0.71075$ Å). The structure
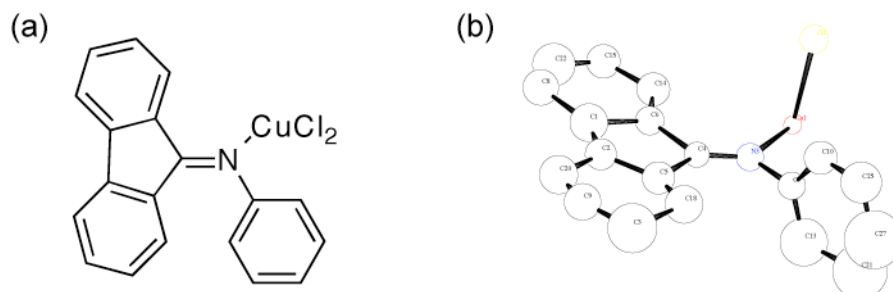
6 Higuchi, M.; Tsuruta, M.; Chiba, H.; Shiki, S.; Yamamoto, K. *J. Am. Chem. Soc.* **2003**, *125*, 9988-9997.

7 Nakajima, R.; Tsuruta, M.; Higuchi, M.; Yamamoto, K. *J. Am. Chem. Soc.* **2004**, *126*, 1630-1631.

8 Imaoka, T.; Tanaka, R.; Arimoto, S.; Sakai, M.; Fujii, M.; Yamamoto, K. *J. Am. Chem. Soc.* **2005**, *127*, 13896-13905.

was solved by a direct method (SHELXS97) on a Dell workstation with the program system CrystalStructure. The structure was refined on F by full-matrix least square methods using 492 reflections within I>2.0 σ (I) and the final R value was 0.130. The atomic parameters are listed in the CIF file.

Figure S3. A chemical structure (a) and crystal structure (b) of the DPA model complex.

The structural information around a copper center in **4CuCl₂-DPAG4** was determined by Cu K-edge X-ray absorption spectroscopy (XAS) of the powder used for the catalysis. The data collection was performed on a Rigaku R-XAS Looper spectrometer with a Ge(311) monochromator used for the energy selection. XAS data was measured in absorption mode up to $k = 15$ Å^{-1}. The data between $k = 3$ Å^{-1} and $k = 12.3$ Å^{-1} was used for the analyses. The DPA model complex (**CuCl₂-(Model)₂**) was used as the reference compound.

Figure S4. (a) EXAFS data (circle) with the fitting results (line) and the (b) Fourier transform of **4CuCl₂-DPAG4** (Blue) and **CuCl₂-(Model)₂** (Green).

The fitting result for the distances of **CuCl₂-(Model)₂**, shown in **Table S1**, is in good agreement with that obtained in the X-ray diffraction data. However, the number of coordination cannot be absolutely defined due to its dependence on the grain size of samples and the resolution of optics system. In addition, the strong correlation with σ_i prevents the definition of absolute value only in the EXAFS fitting. Therefore, we applied the known value of the coordination number obtained from the single crystal data and discussed based on its relative value.

Table S1. Fitting results of the EXAFS data for **4CuCl$_2$-DPAG4** and **CuCl$_2$-(Model)$_2$**.

Sample	Shell	N [a]	R (Å) [b]	ΔE_0 (eV) [c]	δ (Å) [d]	R-Factor [e]
4CuCl$_2$-DPAG4	Cu–N	1.2	1.92	-15.0	0.110	0.006
	Cu–Cl	2.3	2.22	4.99	0.095	
CuCl$_2$-(Model)$_2$	Cu–N	2.0	1.97	-3.86	0.110	0.109
	Cu–Cl	2.0	2.24	8.73	0.095	

[a] Coordination number. [b] Interatomic distance. [c] Edge energy shift from the standard value ($E_0 = 8990$ eV). [d] Debye-Waller factor. [e] The R-factor can be calculated from the following equation.

$$R = \sum \left\{ k^n \chi_{obs}(k) - k^n \chi_{cal}(k) \right\}^2 / \sum \left\{ k^n \chi_{obs}(k) \right\}^2$$

The coordination space around the copper center in **4CuCl$_2$-DPAG4** is very similar to that of the model compound. Differences in the distances for Cu-N and Cu-Cl are within 2 %. Assuming the coordination number of **CuCl$_2$-(Model)$_2$** to be $N_{Cu-N} = 2$ and $N_{Cu-Cl} = 2$, that of the **4CuCl$_2$-DPAG4** was defined to be $N_{Cu-N} = 1.2$ and $N_{Cu-Cl} = 2.3$. Obviously, the number of N-ligand for the dendrimer complex is decreased relative to the model complex. This means that the low flexibility of DPAG4 prevents back-folding of the terminal monomers which would results in multi-site binding. Similar to that of other metallic chloride (e.g. SnCl$_2$, FeCl$_3$ or AuCl$_3$), the complexation between N-ligand in the dendrimer and CuCl$_2$ is determined as 1:1 stoichiometry.

5. Characterization of the Polymer Products

NMR

Soluble part of the polymer products were characterized by ^{1}H, ^{13}C and ^{19}F NMR measurements on an NMR spectrometer (JEOL, JNM-GX400α) using [D$_8$]THF as solvent. ^{1}H NMR (400MHz, C$_4$D$_8$O, δ ppm) 6.90 (d, 2H/monomer), ^{13}C NMR (100MHz, C$_4$D$_8$O, δ ppm) 157.2, 156.8, 126.6, 101,5, ^{19}F NMR (400MHz, C$_4$D$_8$O, δ ppm) –128 ppm.

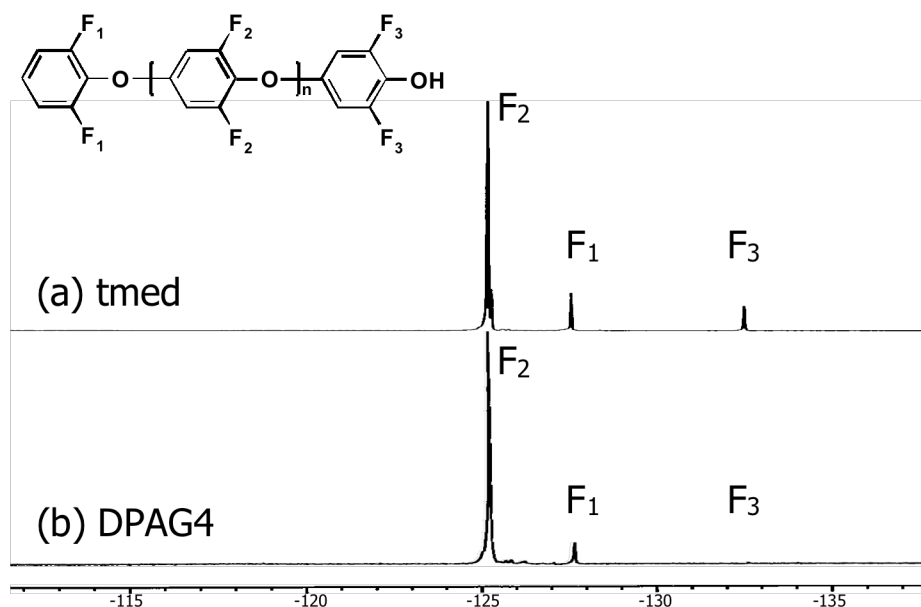**Figure S5.** ^{19}F NMR spectra of F_2PPO products yielded from the catalytic polymerization using (a) CuCl$_2$-TMED and (b) 4CuCl$_2$-DPAG4.

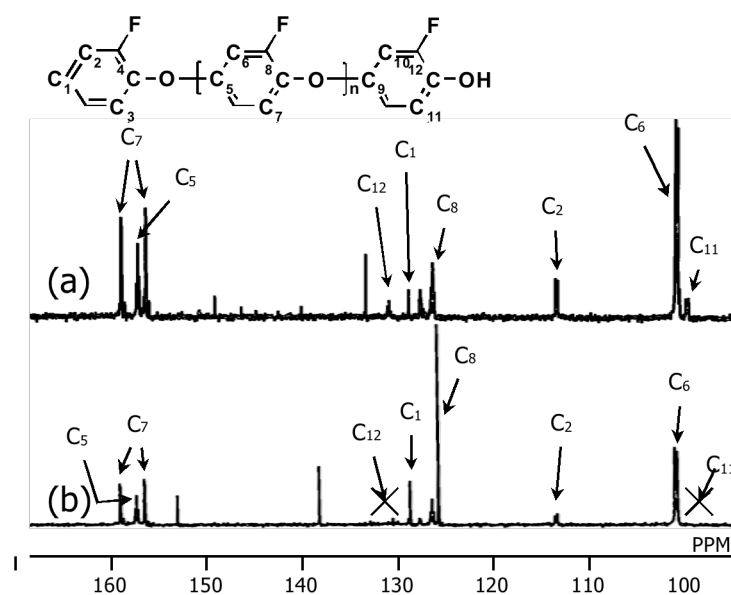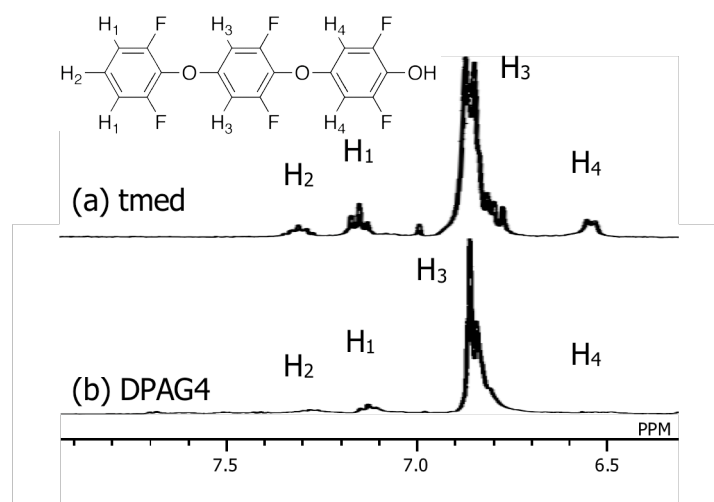**Figure S6.** ^{13}C NMR spectra of F_2PPO products yielded from the catalytic polymerization using (a) CuCl$_2$-TMED and (b) 4CuCl$_2$-DPAG4.

Figure S7. ^{1}H NMR spectra of F_2PPO products yielded from the catalytic polymerization using (a) $CuCl_2$-TMED and (b) $4CuCl_2$-DPAG4.

SEC

Analytical size-exclusion chromatography (SEC) was performed using an HPLC (Shimadzu, LC-10AP) equipped with two tandem SEC columns (Tosoh, TSK-GEL CMHXL and G3000HXL) at 40°C. Tetrahydrofran (THF) was used as the eluent at the flow rate of 1 ml/min. The detection line was connected to a triple detector (Viscotek, TriSEC Model 302) operated at 30 °C. The molecular weights of the dendrimers were calculated from the SEC data which contains refractive index (RI), intrinsic viscosity (IV) and right angle light scattering (RALS) charts in combination with each other. Using this method, we could obtain an exact molecular weight but a converted value against polystyrene.[9]

[9] Bahary, W. S.; Hogan, N. P.; Jilani, M.; Aronson, M. P. In *Advances in Chemistry Series; Chromatographic Characterization of Polymers; Provder*, T., Barth, H. G., Urban, M. W., Eds.; American Chemical Society: Washington, D. C., 1995; Vol. 247, p 151-166.
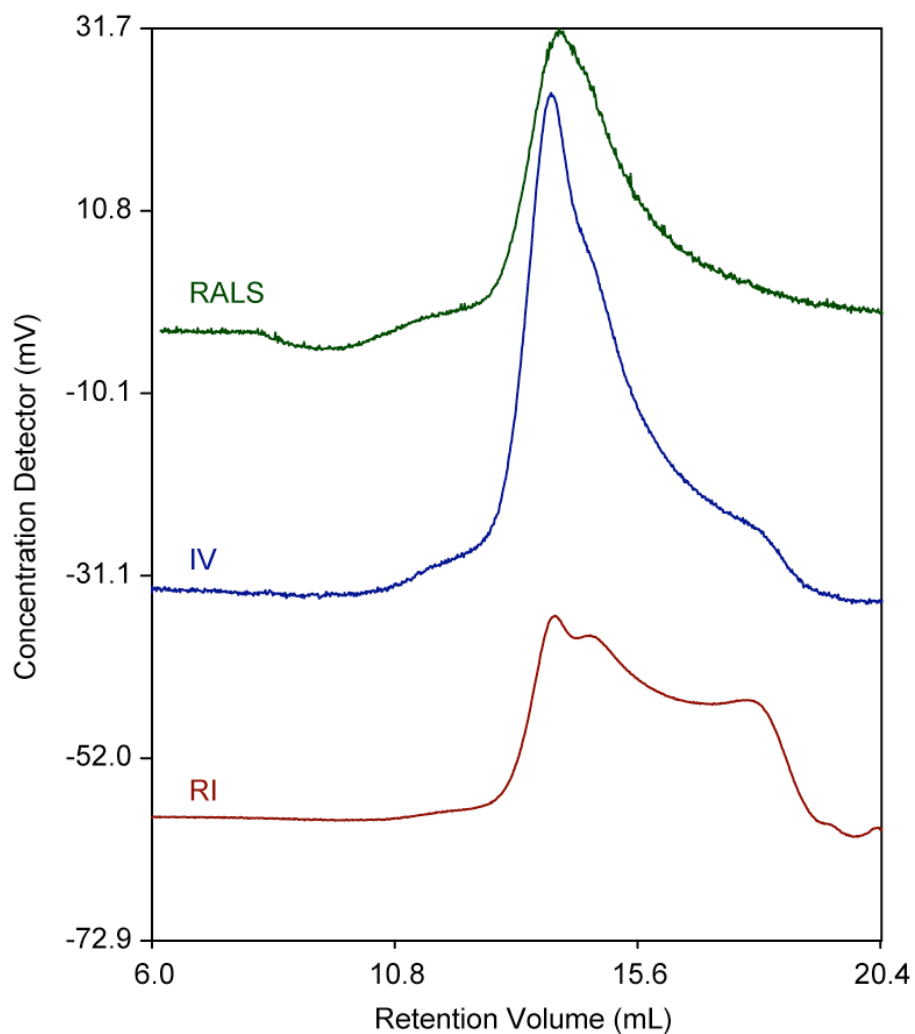
Figure S8. GPC traces of as polymerized F$_2$PPO measured by RALS, IV and RI detectors. The polymerization was carried out using the dendrimer complex (Entry 2).
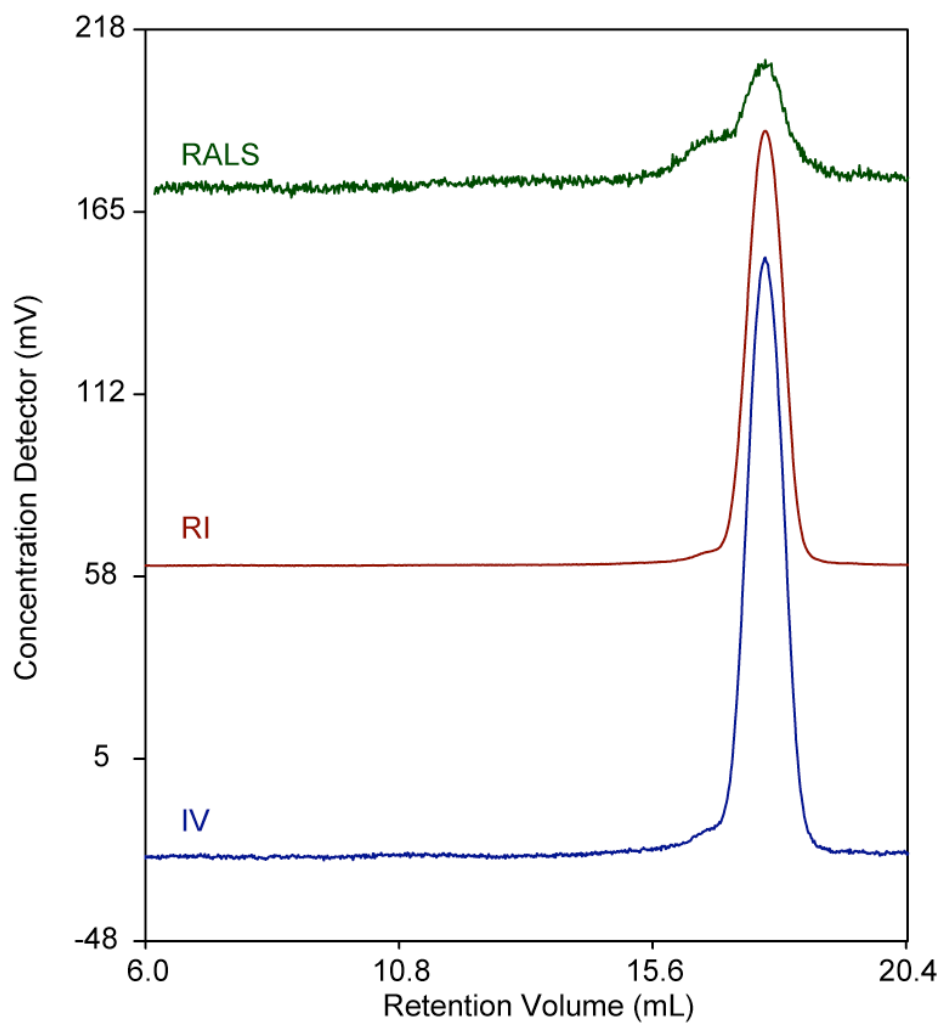
Figure S9. GPC traces of isolated F_2PPO (low molecular weight) measured by RALS, IV and RI detectors. The polymerization was carried out using the dendrimer complex (Entry 2).

6. Monitoring the Reaction Progress

During the polymerization of 2,6-difluorophenol, the conversion of monomers vs. reaction time was monitored by GC (gas chromatography) analysis. The GC analysis was performed on a gas chromatograph (Shimadzu, GC-14B) using a TCD detector. A packed glass-column (Shinwa-kakou, Silicone DC 200) was used for the analysis. The results were shown in the Figure S10.
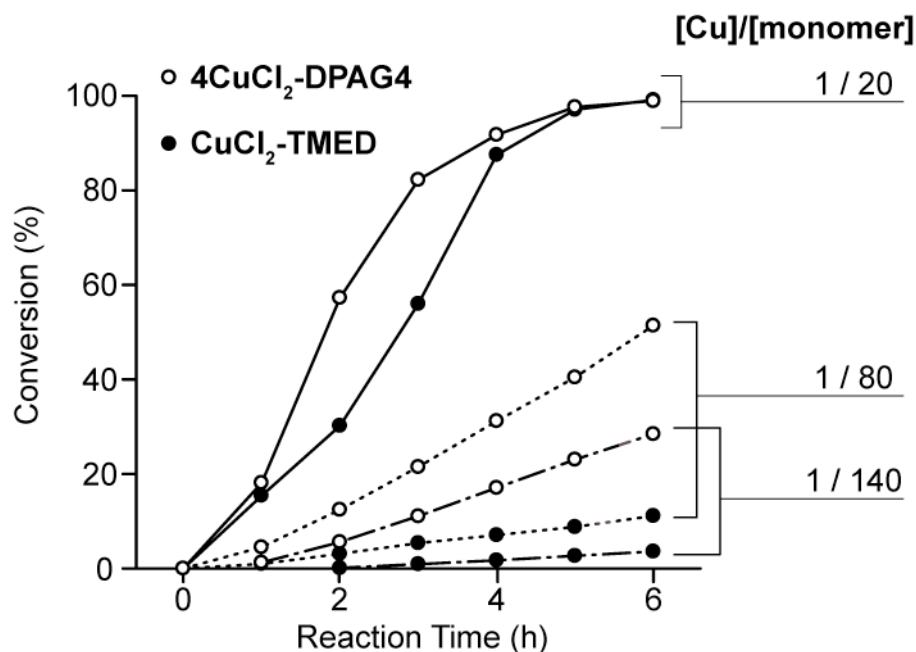

Figure S10. Conversion (%) of the monomer vs. reaction time. A reaction progress for the polymerization using DPAG4 or TMED complex at different concentration of the copper. The measurement was carried out by direct injection of the reaction mixture into GC at every reaction time.

At the initial stage of polymerization, the reaction progress was also monitored using ^{19}F NMR in which each signal, attributed to the monomer and three different parts of polymer, can be individually recognized. Total turn-over-number (TON) was calculated from the following equation;

$$[TON] = \frac{C^0_{monomer}}{C^0_{Cu}} \times \frac{I_{F1} + I_{F2}}{I_{F1} + I_{F2} + I_{F3} + I_{Fmono}} \quad (1)$$

where $C^0_{monomer}$ and C^0_{Cu} are the initial molar concentration of monomers and copper complexes. The integrals of each ^{19}F signal (I_{F1}, I_{F2}, I_{F3} and I_{Fmono}) are corresponding to fluorine atoms (F$_1$, F$_2$, F$_3$ and F$_{mono}$) as shown in Figure S11.

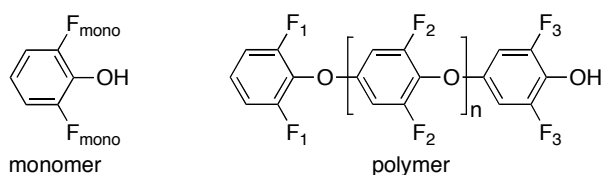**Figure S11.** Fluorine atoms in the monomer and polymer (F2PPO).

The TON obtained at each reaction time up to 6 h is shown in Figure S12. In addition, turnover-frequency (TOF) for each catalytic system was determined from the slope of TON (Table S2).
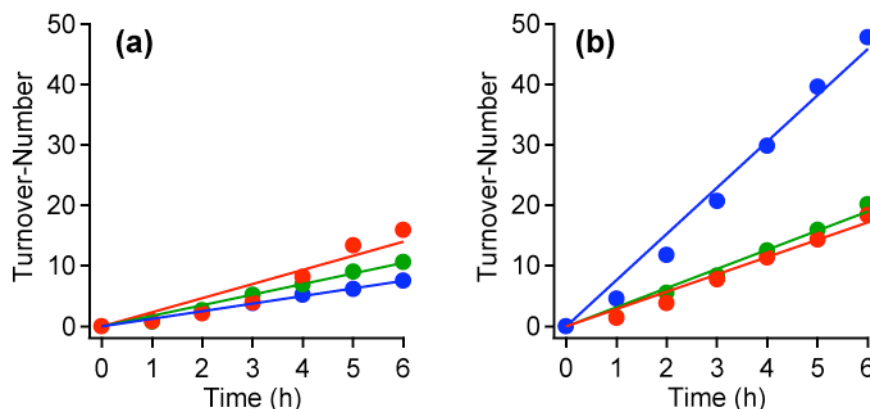

Figure S12. Accumulated turnover-number at each reaction time for (a) CuCl-TMED (containing 0.25 mol L^{-1} Ph_2Py) and (b) $4CuCl_2$-DPAG4 (without Ph_2Py). The initial concentration of monomer was 0.5 mol L^{-1} (1 mmol in 2 mL) for all experiments. The catalyst concentration was varied based on the [Cu]/[monomer] ratio of (Red) 1/20, (Green) 1/80 and (Blue) 1/140. All other conditions were the same as the **Entry 1** system.

Table S2. Turnover-frequency determined at 6 hours after the reaction start for each catalytic system.

[CuCl$_2$]/[monomer]	CuCl$_2$-TMED	4CuCl$_2$-DPAG4
1/20	2.33	2.85
1/80	1.74	3.17
1/140	1.25	7.63

7. Redox Behavior and Electron Transfer

The redox potentials of copper complexes attributed to the Cu(II)/Cu(I) redox couple were characterized by cyclic voltammetry measurements. All measurements were performed in nitrobenzene (5 mL) in the presence of 0.2 mol L^{-1} tetra-n-butylammonium perchlorate ([Bu$_4$N][ClO$_4$]) as a supporting electrolyte. Before the measurements, all the sample solutions were deaerated by N_2 bubbling for 5 min. Details for each sample is shown below. A glassy carbon electrode (GCE, ϕ = 3 mm) was used as a working electrode. An Ag/Ag$^+$ electrode (an Ag wire in acetonitrile solution containing 0.01 mmol L^{-1} $AgNO_3$ + 0.1 mol L^{-1} [Bu$_4$N][ClO$_4$]) was used as a reference electrode. A platinum wire was used as a counter electrode. The scan rate was set to 0.1 V s^{-1}.

Sample 1. [4CuCl$_2$-DPAG4]: CuCl$_2$ (0.68 mg) and DPAG4 (6.8 mg) were dissolved in 5 mL nitrobenzene containing 0.2 mol L^{-1} [Bu$_4$N][ClO$_4$].

Sample 2. [CuCl$_2$-2Model]: CuCl$_2$ (0.68 mg) and Model (1.29 mg) were dissolved in 5 mL nitrobenzene containing 0.2 mol L^{-1} [Bu$_4$N][ClO$_4$].

Sample 3. [CuCl$_2$-tmed]: CuCl$_2$ (0.68 mg) and tmed (0.59 mg) were dissolved in 5 mL nitrobenzene

containing 0.2 mol L^{-1} [Bu$_4$N][ClO$_4$].

Sample 4. [CuCl$_2$-Py]: CuCl$_2$ (0.68 mg) and pyridine (100 mg) were dissolved in 5 mL nitrobenzene containing 0.2 mol L^{-1} [Bu$_4$N][ClO$_4$].
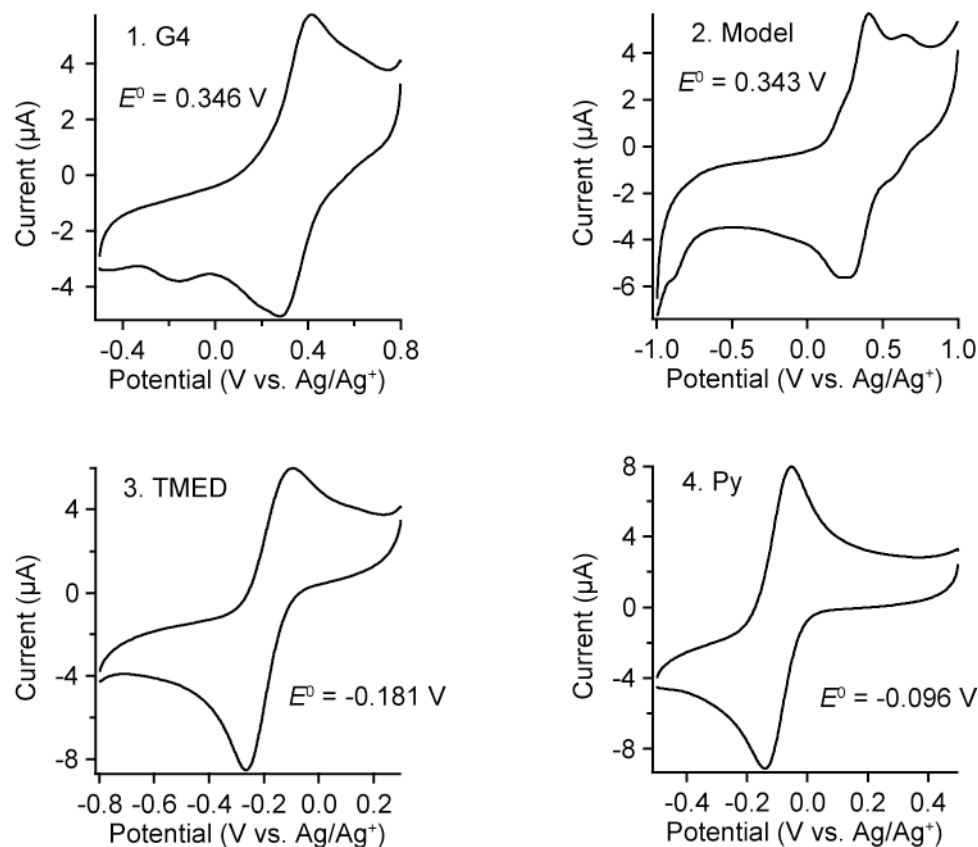

Figure S13. Cyclic voltammograms of the copper complexes of various N-ligands. The redox potential (E^0) shown in the figures was determined as the midpoint between cathodic and anodic peaks.

Kinetic trace for the electron transfer reaction between the copper complex and phenols (eq. 2)was monitored in UV-vis absorption change as reported by Tsuchida et al.[10] The monitor wavelength is 800 nm at which characteristic d-d absorption band of Cu(II)-L was observed.
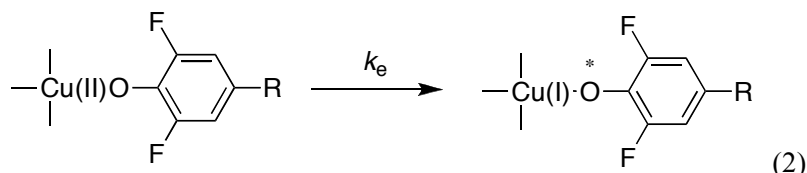
General procedure for the analysis is as below. The solution of copper complexes (5 mmol L^{-1}) in nitrobenzene (3 mL) was prepared. On the other side, the solution of 2,6-difluorophenol (0.2 mol L^{-1}) and Ph$_2$Py (0.2 mol L^{-1}) was also prepared in nitrobenzene. Before the analysis, these solutions were deaerated through repetitions of freezing and N$_2$ substitution for several times. They were mixed with

10 Tsuchida, E.; Nishide, H.; Nishiyama, T. *Makromol. Chem.* **1975**, *176*, 1349-1358.

each other in an enclosed Thunberg tube, and then transferred to a quartz cell with 1 cm optical path-length. The absorption spectrum was measured repeatedly with an interval of 5 seconds. After 10 hours, the spectrum was measured again as an end-point of the reaction. Because an excess amount of the phenols was added to the solution, the reaction was analyzed as pseudo-first order. The observed rate constants as first order reaction is as shown in Table S3.

Table S3. Rate constants of the electron transfer step for copper complexes.

Complex	k_e (min^{-1})
4CuCl$_2$-DPAG4	0.0104
CuCl$_2$-2Model	0.0094
CuCl$_2$-tmed	0.0068
CuCl$_2$-Py	0.00097

These results indicate that the phenylazomethine compounds (including model complex and dendrimer G4 complex) have relatively strong oxidizing power to the phenol derivatives. However, they are insufficient to explain the high catalytic activity of G4 dendrimer. Indeed, the G4 dendrimer shows much higher activity than the model complex, even though both the electron transfer and redox potential are identical to each other. The answer to the question is provided from the concentration dependence of the TOF. While the TOF of mono-nuclear complex such as TMED seriously dropped with the concentration decreasing, the dendrimer complex retained the TOF even at very low concentration (Cu/monomer = 1/140). This could be explained by the concentration effect of copper complexes in the dendritic nanocapsule. In addition, the concentration effect of bases should be indispensable for the efficient catalysis because the generation number dependence (Figure 1a in the main text) shows drastic enhancement of the activity at n = 4. In summary, we decided that all-in-one encapsulation in a nanoscale dendrimer capsule is the best arrangement for the catalysis.

Acknowledgement